IEEE Access
Multidisciplinary : Rapid Review : Open Access Journal

Received 9 August 2022, accepted 10 October 2022, date of publication 19 October 2022, date of current version 27 October 2022.

Digital Object Identifier 10.1109/ACCESS.2022.3215759

RESEARCH ARTICLE

A Maximum Localization Rate Algorithm for 3D Large-Scale UWSNs

JIA SONG[1], HUILONG JIN[1], XIAOBO SHEN[2], AND SHUJING ZHANG[3]
[1]College of Engineering, Hebei Normal University, Shijiazhuang 050024, China
[2]Bluestar Engineering Company Ltd., Beijing 101318, China
[3]Beijing Dewei Jiaye Technolngy Company Ltd., Beijing 101300, China

Corresponding author: Shujing Zhang (shujing_zhang@yeah.net)

This work was supported in part by the National Natural Science Foundation of China under Grant 61701165, Grant 61771181, and Grant 61501168; in part by the Natural Science Foundation of Hebei Province under Grant F2016205182; and in part by the Project of Science and Technology Development Center in Higher Education Institutes of the Ministry of Education under Grant 2021LDA06003.

ABSTRACT Underwater wireless sensor networks (UWSNs) play an increasingly important role in monitoring the marine environment. The research of sensor node localization is one of the biggest concerns in UWSNs, but there are still many formidable obstacles to overcome, including localization accuracy, localization rate, and other issues. In contrast to localization accuracy, however, few studies focus on increasing the node localization rate. Therefore, this paper proposes a maximum localization rate (MLR) algorithm for 3D large-scale UWSNs. In view of the number of anchor nodes around the unknown node, the MLR algorithm designs different positioning strategies, such as the triangular cosine method and the dynamic position-assisted localization method. The MLR algorithm also adopts the regular tetrahedron network topology and the collinear judgment mechanism to guarantee localization accuracy. The simulation results demonstrate that excluding isolated nodes, the MLR algorithm can achieve the maximum localization rate while maintaining a certain level of positioning accuracy at the same time.

INDEX TERMS Underwater wireless sensor networks, underwater sensor node localization, localization rate, localization accuracy, TOA.

I. INTRODUCTION

Underwater wireless sensor networks (UWSNs) have been widely applied in several domains in recent years, including marine disaster prediction, underwater environment monitoring, marine resource exploration, and so on. UWSNs have a huge impact on how people learn about the ocean. Fig. 1 shows the standard three-dimensional (3D) model of UWSNs. Surface buoys use satellites to receive position data and transmit the data collected by underwater sensor nodes to the base station. The base station is responsible for collecting, processing, integrating, and transmitting the data information to the satellite. The anchor node and unknown node comprise the majority of underwater sensor nodes. The sensor node that knows its position in advance is referred to as the anchor node, and its function is to assist the unknown node positioning. On the other hand, the unknown node is mainly used to collect relevant information of the monitoring area and requires position estimation. Neighbor nodes are those when the measured distance between two nodes is less than the communication radius. When there are no neighbor nodes around a node, it is called an isolated node. Instead, it is referred to as a valid node. Underwater sensor nodes are all equipped with air pumps and anchored to the seafloor by cables of different lengths. The depth of the sensor node can be adjusted by modifying the cable length and the underwater pressure sensor can be used to measure it. As a result, the 3D localization of sensor nodes can be converted to two-dimensional (2D) planar positioning when needed.

Positioning technology has attracted extensive attention since it is the foundation and a fundamental component of UWSNs. Unlike terrestrial wireless sensor network (WSN), adverse underwater environments such as water currents, human activities, and underwater creature contacts will result in node mobility [2]. Moreover, communication between nodes in the marine environment will be impeded by the

The associate editor coordinating the review of this manuscript and approving it for publication was Sun-Yuan Hsieh.

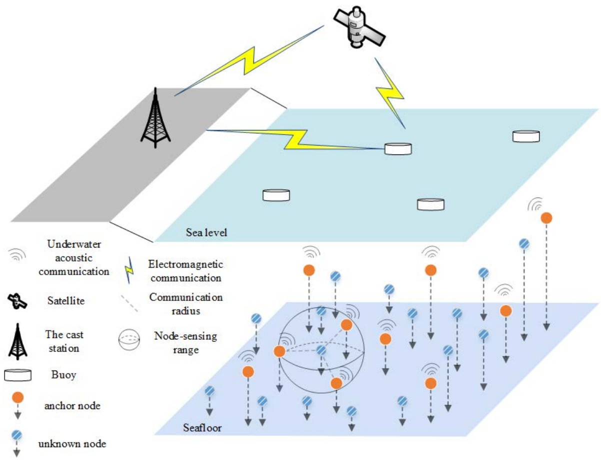

FIGURE 1. Three-dimensional model of UWSNs.

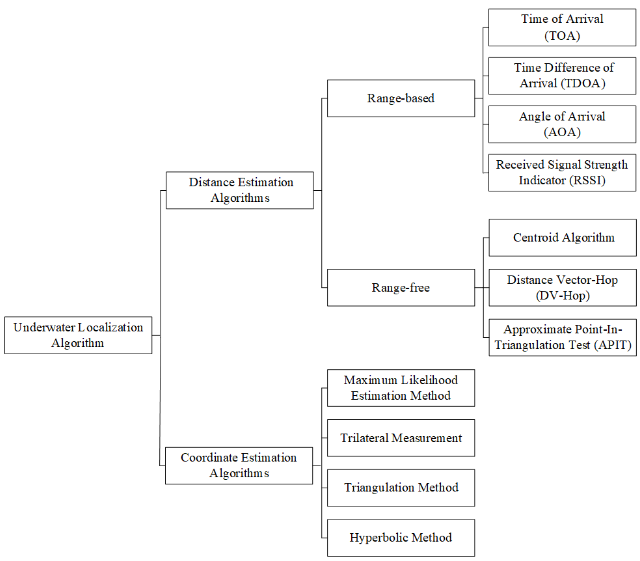

FIGURE 2. Underwater localization algorithm.

underwater acoustic channel. The particularity and uncertainty have brought forth huge hurdles for node localization in UWSNs.

Generally speaking, the two steps of an underwater localization algorithm are distance estimation and coordinate estimation. As shown in Fig. 2, first, the correlation algorithm is used to estimate the distance between the unknown node and the anchor node. The unknown nodes' coordinates are then resolved using the estimated distance. Distance estimation algorithms can be categorized into range-based and range-free depending on whether the distance value needs to be measured. Range-based localization methods that are frequently employed include Time of Arrival (TOA) [3], [4], Time Difference of Arrival (TDOA) [5], [6], Angle of Arrival (AOA) [5], [7], and Received Signal Strength Indicator (RSSI) [8], [9], while range-free algorithms include Centroid Algorithm [10], Distance Vector-Hop (DV-Hop) [11], [12], and Approximate Point-In-Triangulation Test (APIT) [13], etc.

Once the distance between nodes is obtained, coordinate estimation is required. There are numerous methods of coordinate estimation, including the maximum likelihood estimation method, trilateral measurement, triangulation method, hyperbolic method, and others. To locate the unknown node in a 2D UWSN, at least three non-collinear anchor nodes are needed. The aforementioned requirements cannot, however, be met by every anchor node in the network. For example, the unknown node at the edge of a spatial region usually contains only one or two neighbor anchor nodes. The aforementioned approach cannot estimate the node coordinate in the given condition, hence the unknown node fails to be located. Due to factors like high cost, complex environment, and challenging deployment for underwater sensor nodes, the node density of UWSNs is typically lower than that of WSN. This eventually results in a greater number of unknown nodes that cannot be located, which inevitably leads to the low node localization rate of UWSNs. Based on these factors, this paper proposes a maximum localization rate (MLR) algorithm for 3D large-scale UWSNs. In this scheme, as long as the unknown node is not isolated (i.e. the number of neighbor anchor nodes around the unknown node is not less than 1), this approach can successfully perform localization estimation.

The major contributions of this paper are as follows:

1) Based on the number of anchor nodes surrounding the unknown node, the MLR algorithm designs different positioning strategies. When four or more neighbor anchor nodes surround an unknown node, the MLR algorithm adopts the traditional method to locate nodes in 3D space. When there are less than four neighbor anchor nodes, the nodes are projected from 3D space to 2D space to estimate coordinates. In addition, the regular tetrahedron deployment is adopted in the MLR algorithm network topology to take the accuracy performance of node positioning into account.

2) The underwater node location will exist in coplanar or collinear phenomena in both 3D and 2D space, therefore there is no one-of-a-kind method for estimating the location of unknown nodes. To solve this problem, a collinear judgment mechanism is designed in this paper. This method preprocesses the anchor node before estimating the coordinates of the unknown node to avoid the influence of collinearity on positioning accuracy.

3) An effective triangular cosine method is proposed to address the situation when an unknown node has two neighbor anchor nodes. To improve the localization accuracy, an anchor node is selected from non-neighbor anchor nodes to form an approximately equilateral triangle with the other two neighbor anchor nodes. To obtain the 2D projection distance between the unknown node and the optimal non-neighbor anchor node, this method additionally analyzes the position relationship between the nodes, and it summarizes a straightforward and adaptable triangular cosine method. The unknown node can thus be successfully located in the 2Dplane using two neighbor anchor nodes, an optimal non-neighbor anchor node, and the projected distances between the unknown node and these three nodes mentioned above.

4) This paper also proposes a dynamic position assisted localization method based on the mobility of the anchor node to cope with the situation when an unknown node only has one neighbor anchor node. Based on the 3D movement model of the anchor node, by analyzing the anchor node's locations that are recorded as the node moves over time, the dynamic position of the anchor node that is farthest from its static position is chosen. The static position and the dynamic position are then virtualized as two independent anchor nodes, and the coordinates of the unknown node can be estimated by using the aforementioned triangular cosine method.

The rest of the paper is arranged as follows: In Section 2, we survey the literature review of the related localization algorithms. The MLR algorithm is introduced in Section 3. In Section 4, the simulation results and analysis are discussed. Finally, Section 5 provides conclusions.

II. RELATED WORK

The existing localization algorithms for 3D UWSNs mainly focus on reducing the localization error, but few researchers emphasize increasing the localization ratio. Localization algorithms can be further divided into static positioning algorithms and dynamic positioning algorithms depending on whether the node moves or not. Static positioning algorithms include UPS, LSLS, 3DUL, etc. While dynamic positioning algorithms predict the positions of anchor nodes by analyzing the node mobility, such as Scalable Localization scheme with Mobility Prediction (SLMP) and Mobility Prediction and Particle Swarm Optimization (MP-PSO). The goal of both static and dynamic localization algorithms is to increase the node localization rate. The LSLS algorithm [14] improves the UPS [15] positioning scheme. In the first stage, unknown nodes on the node controlling area of the sea surface are located. In the second stage, the nodes that have been located in the first stage are regarded as reference nodes. Combined with anchor nodes, the unknown nodes that remained can be identified iteratively. If a node fails to be localized in the first two phases, it can initiate a location request in the third phase. The to-be-localized area of the node will then be localized using a new group of anchors that will cover as much of it as possible while maximizing the communication range. This algorithm increases the positioning rate, but the communication in the last two stages is so frequent that it may cause high energy consumption. In [16], a localization algorithm called Three-Dimensional Underwater Localization (3DUL) is proposed. In this study, only three anchor nodes are needed for positioning at first, and then the positioned nodes are upgraded as reference nodes which are used for unknown nodes that remained to be localized. It increases the node coverage, but the problem is that step-by-step positioning may result in error accumulation. The nodes deployed in the underwater wireless sensor network will move as a result of tidal interference and other environmental conditions, which lowers the accuracy rate of the static positioning algorithm. Therefore, the dynamic positioning algorithm develops as needed. In Reference [17], the authors propose a scalable asynchronous localization algorithm with mobility prediction (SLMP). It analyses the asynchronous communication between the anchor nodes and ordinary nodes, then, the original position of ordinary nodes is acquired and the future position of ordinary nodes is predicted and updated. Accordingly, it upgrades the ordinary nodes which are precisely located to reference nodes. Besides, the new reference nodes locate the other unknown ordinary nodes together with the anchor nodes until the end of localization. The algorithm has a high localization ratio, but the localization error is still large because iterative positioning will lead to error accumulation. In [18], a mobility prediction and particle swarm optimization algorithm (MP-PSO) is presented. Firstly, a range-based particle swarm optimization algorithm is used to locate the beacon node by measuring the distance from the node to the surface buoy. Then, the location of the unknown node at the next time can be predicted by estimating the velocity of the unknown node. However, a time goes on, the node localization error is also enlarged, which means it cannot reach the confidence threshold and may lead to inefficient node localization. In [19], this paper proposes a movement prediction location (MPL) algorithm. In this algorithm, the TOA strategy is proposed firstly, and the buoy node is used to locate the primary nodes. The secondary nodes are then optimally located using the primary nodes through dimension-reduced processing and the grey wolf optimizer. Finally, the node position is obtained, and the node movement prediction stage is initiated. This algorithm enables some nodes that cannot be located to self-locate, and the node localization rate is improved correspondingly, but the complexity is relatively high since the grey wolf optimization is used in selecting anchor nodes [20] presents a mobility-assisted localization scheme with a time synchronization-free feature (MALS-TSF). The algorithm is divided into two phases. In the first part, based on the mobility of beacon nodes, a localization scheme is proposed to calculate the distances between nodes. Then, the coordinates of some unknown nodes are then determined using this scheme. Following that, reference nodes are selected for the second part based on the setting of confidence degree. In the second part, the two-way TOA method is used to obtain the distances between nodes, and the reference nodes are used to locate the remaining unknown nodes. However, this method does not consider the localization of edge nodes. In [21], A node positioning method based on dynamic node selection and mobile prediction (NDSMP) is introduced. Anchor nodes are used to predict node motion. Each anchor node serves as a reference node, and common nodes whose confidence value is well above the confidence threshold may also serve in this capacity. The common node dynamically selects the location algorithm based on its node density for location calculation after getting the information from the reference node. This method can effectively solve the problems of network edge and network void, as well as improve the positioning rate, but the coordinate estimation model utilized will lead to a large error. Reference [22] proposed a mobile-beacon based iterative localization (MBIL) mechanism. The algorithm first

TABLE 1. Comparison of range measurement methods.

Ranging techniques	Advantages	Disadvantages
RSSI	no need for extra hardware support	low localization accuracy
One-way TOA	high localization accuracy	requirement for precise time synchronization
Two-way TOA	no need of time synchronization and high localization accuracy	higher implementation cost
TDOA	high positioning accuracy	requirement for extra hardware support
AOA	high positioning accuracy	requirement for special antenna array

uses mobile beacon nodes to locate adjacent sensor nodes. The sensor node evaluates its confidence after receiving the location data to ascertain if it qualifies as a reference node. Then, the unknown nodes locate three adjacent reference nodes with the highest evaluation index, and the remaining unknown nodes are then iteratively located. The calculation method can effectively improve the node localization rate, but the computational cost rises when the reference node evaluation index is calculated repeatedly.

To sum up, the dynamic and static positioning algorithms, to a certain extent, improve the localization rate of unknown nodes by using the iteration method. However, the iteration method is imperfect at handling node marginalization and error accumulation due to its high computational complexity. Therefore, this paper proposes a maximum localization rate (MLR) algorithm for 3D large-scale UWSNs.

III. LOCATION ALGORITHM ANALYSIS

The maximum localization rate algorithm consists of two parts: the first part is the distance estimation, and the other is the coordinate estimation. The following is a detailed introduction of the two parts mentioned above.

A. NETWORK MODEL

As shown in Fig. 3(a), anchor nodes (the orange points) are deployed randomly in a 3D monitored region. In UWSNs, the random deployment is the main choice for most of practical applications. For the last decade, researchers have also designed the regular tetrahedron deployment scheme (anchor nodes are deployed at the vertices of some prepositioned regular tetrahedrons, as shown in Fig. 3(b)) and the cube deployment scheme (as shown in Fig. 3(c), anchor nodes are deployed at the vertices of the prepositioned space-filling cubes). It has been proved that the regular tetrahedron deployment has better performance than the cube deployment and the random deployment scheme in terms of increasing localization ratio and reducing localization error [23]. Therefore, this paper chooses to deploy anchor nodes at the vertices of some prepositioned regular tetrahedrons and unknown nodes in the 3D monitored space randomly. The network model is composed of N sensor nodes, in which the number of anchor nodes is n and the number of unknown nodes is m. It is assumed that the communication radius of all sensor nodes is R and the side length of a regular tetrahedron is L.

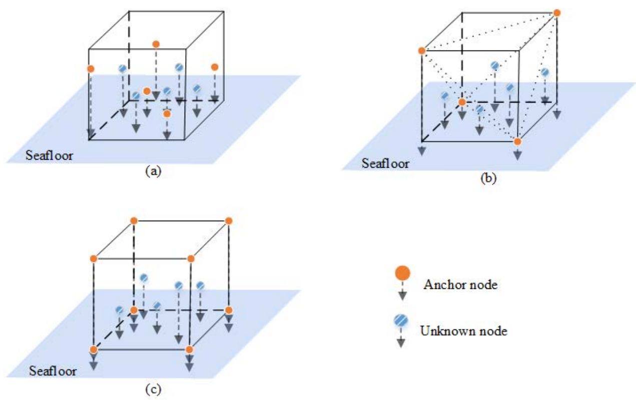

FIGURE 3. Network model.

B. DISTANCE ESTIMATION

1) COMPARISON OF DISTANCE ESTIMATION ALGORITHMS

In the introduction part, the range-based and range-free localization methods are briefly elucidated. Range-based localization methods provide a precise location of the sensor node while range-free localization methods can only estimate the location roughly. Therefore, range-based localization methods are adopted in this paper. The advantages and disadvantages of the four range-based algorithms are listed in Table 1. Besides, TOA is subdivided into one-way TOA and two-way TOA. Through comparative analysis, the two-way TOA proves to be better performed in time synchronization and localization accuracy, it is hence applied in the study of the underwater acoustic sensor network.

2) TWO-WAY TOA ALGORITHM

It is of great necessity to estimate the travel time between two sensor nodes based on the two-way TOA. As is shown in Fig. 4, a packet containing the sending time t_0 and its own ID to

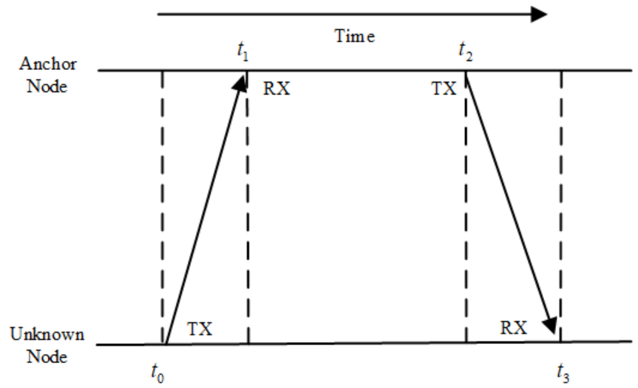

FIGURE 4. The two-way TOA.

the surrounding anchor nodes is sent by the unknown node. When an anchor node receives the packet at time t_1, after an interval of time, it will feed back to the unknown node a packet containing its location and time information at time t_2. Finally, the unknown node receives the feedback at time t_3. Therefore, the estimated distance between the unknown node and the anchor node can be got by the following equation:

$$D = \frac{(t_1 - t_0) + (t_3 - t_2)}{2} \cdot c \tag{1}$$

The propagation speed c of the underwater acoustic signal can be calculated as follows:

$$\begin{aligned} c(T, S, Z) = {} & 1449.2 + 4.6T - 0.055T^2 + 0.00029T^3 \\ & + (1.34 + 0.01T)(S - 35) + 0.016Z \end{aligned} \tag{2}$$

where T represents the medium temperature of the underwater acoustic signal in the propagation process in degrees Celsius, S represents the medium salinity of underwater acoustic signal in the propagation process, in parts per thousand, and Z represents depth in meters. According to (2), the propagation speed in the seawater is influenced by many parameters, such as salinity, temperature, and depth. Therefore, in the latter part of this paper, to stimulate the propagation speed of acoustic waves in real underwater environments, the average medium temperature and average medium salinity in the shallow water area of the Bohai Sea in summer are selected for modeling.

C. CASE ANALYSIS

The collinearity phenomenon will happen, when the neighbor anchor nodes are located in a straight line for the 2D environment and in the same plane for the 3D space [24]. The collinear problem will result in solutions that are not unique for estimating the location of unknown nodes. There are mainly three situations for approximate collinearity in a 2D environment: when three and above anchors are almost in a straight line; when the relative position of any two anchors is too close, while they are also far from the unknown nodes; when the three anchors are all nearby and no matter what triangular shape that they compose is, meanwhile, unknown nodes have a further distance to them. Similarly, in a 3D environment, if four or more neighbor anchor nodes are in the same plane, there exist two node locations, hence it is impossible to locate the unknown node definitely. Therefore, to solve the collinear problem, the following four steps are preprocessed before estimating the location:

1) If the neighbor anchor nodes are situated in the same plane, choose three nodes randomly.
2) When the three anchor nodes are projected onto the 2D plane where the unknown node is located, the cosine value of the three included angles of the triangle formed by the three anchor nodes is compared with the threshold value to judge if the three anchor nodes are approximately collinear. If collinear, two of the three anchor nodes' information will be randomly reserved.
3) When no less than one neighbor anchor node is projected to the same coordinate on the 2D plane where the unknown node is located, only the 2D plane position information of one anchor node is retained.
4) If neighbor anchors do not have the problems mentioned above, their location information will be saved directly. The number of neighbor anchor nodes after preprocessing is recorded as K.

Suppose that K neighbor anchor nodes remain after preprocessing. The coordinate estimation can then be divided into four separate situations, that is, $K >= 4$, $K = 3$, $K = 2$ and $K = 1$ respectively.

D. COORDINATE ESTIMATION

1) $K >= 4$

It is assumed that there are k neighbor anchor nodes (such as A, B, C, D, E, F, as shown in Fig. 5) around the unknown node P, whose coordinates are respectively (x_1, y_1, z_1), $(x_2, y_2, z_3), \cdots, (x_k, y_k, z_k)$, $K >= 4$, then, four anchor nodes are randomly chosen to determine whether their locations constitute a regular tetrahedron. The search stops once the four neighbor anchor nodes $A\left(x_{c_1}, y_{c_1}, z_{c_1}\right)$, $B\left(x_{c_2}, y_{c_2}, z_{c_2}\right)$, $C\left(x_{c_3}, y_{c_3}, z_{c_3}\right)$, $D\left(x_{c_4}, y_{c_4}, z_{c_4}\right)$ that make up the regular tetrahedron are found (as shown in Fig. 5(a)), and the coordinates of the unknown node will be estimated by the formula (3)-(8). If the four neighbor anchor nodes that constitute the regular tetrahedron cannot be found after traversing all kinds of the C_K^4 possibilities (as shown in Fig. 5(b)), the unknown node will be located using the traditional method. Namely, all K anchor nodes are used to estimate the coordinates of unknown nodes according to the formula (3)-(8).

Suppose that the distances between the unknown node $P(x_P, y_P, z_P)$ and the anchor nodes are $D_1, D_2, \cdots, D_k$; the depths of nodes, namely z_1, z_2, $\cdots z_k$ and z_P are acquired by an equipped pressure sensor. According to the Euclidean distance formula:

$$(x_P - x_i)^2 + (y_P - y_i)^2 + (z_P - z_i)^2 = D_i^2 \tag{3}$$

There $i = 1, 2, \cdots, k$.

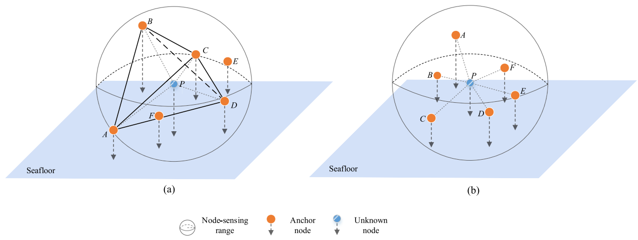

FIGURE 5. The position relation between anchor node and unknown node of $K >= 4$.

Let

$$A = \begin{bmatrix} 2(x_1 - x_k) & 2(y_1 - y_k) \\ \vdots & \vdots \\ 2(x_{k-1} - x_k) & 2(y_{k-1} - y_k) \end{bmatrix} \tag{4}$$

$$B = \begin{bmatrix} D_k^2 - D_1^2 + x_1^2 - x_k^2 + y_1^2 - y_k^2 + (z_1 - z_k)^2 \\ \vdots \\ D_k^2 - D_{k-1}^2 + x_{k-1}^2 - x_k^2 + y_{k-1}^2 - y_k^2 + (z_{k-1} - z_k)^2 \end{bmatrix} \tag{5}$$

$$AX = B \tag{6}$$

$$X = \begin{bmatrix} x_P \\ y_P \end{bmatrix} \tag{7}$$

We canhave

$$X = (A^T A)^{-1} A^T B \tag{8}$$

Finally, the estimated horizontal coordinates of the unknown nodes can be calculated, namely, $X_P = X(1)$, $Y_P = X(2)$.

2) $K = 3$

If an unknown node obtains three projected distances from different anchor nodes, it can transform the 3D spatial localization of sensor nodes into 2D planar localization by. As is shown in Fig. 6, the coordinates of the three anchor nodes are $A(x_1, y_1, z_1)$, $B(x_1, y_1, z_1)$, and $C(x_1, y_1, z_1)$, the projections of the anchor nodes on the plane of the unknown node are $A'(x_1, y_1)$, $B'(x_2, y_2)$, and $C'(x_3, y_3)$, and the coordinate of the node to be located is $P(x_P, y_P)$. The distances between the unknown node P and the three anchor nodes A, B, C are D_1, D_2, D_3.

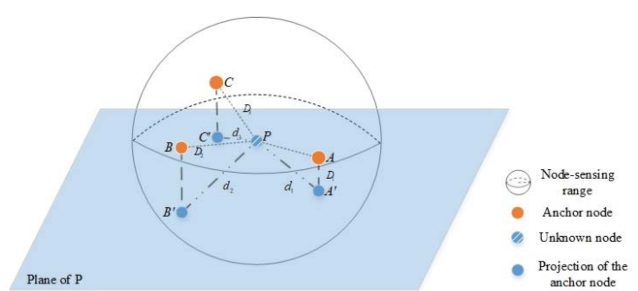

FIGURE 6. The position relation between anchor node and unknown node of $K = 3$.

According to the Pythagorean theorem, the distance from the unknown node P to the anchor nodes A', B', C' are d_1, d_2, d_3, which can be calculated by:

$$d_i = \sqrt{D_i^2 - (z_i - z_p)^2} \tag{9}$$

There $i = 1, 2, 3$.

Then, the distances between the unknown node $P(x_P, y_P)$ and anchor nodes $A'(x_1, y_1)$, $B'(x_2, y_2)$, $C'(x_3, y_3)$ are:

$$(x_P - x_i)^2 + (y_P - y_i)^2 = d_i^2 \tag{10}$$

There $i = 1, 2, 3$.

Transpose the formula:

$$-2x_i x_P - 2y_i y_P + r = d_i^2 - r_i \tag{11}$$

Then

$$A = \begin{bmatrix} -2x_1 & -2y_1 & 1 \\ -2x_2 & -2y_2 & 1 \\ -2x_3 & -2y_3 & 1 \end{bmatrix} \tag{12}$$

$$B = \begin{bmatrix} d_1^2 - r_1 \\ d_2^2 - r_2 \\ d_3^2 - r_3 \end{bmatrix} \tag{13}$$

$$X = \begin{bmatrix} x_P \\ y_P \\ r \end{bmatrix} \tag{14}$$

We can get

$$X = (A^T A)^{-1} A^T B \tag{15}$$

Finally, the estimated horizontal coordinates of the unknown nodes can be calculated, namely, $X_P = X(1)$, $Y_P = X(2)$.

3) $K = 2$

When the unknown node is surrounded by two neighbor anchor nodes, an effective triangular projection locating method is proposed in this paper. Firstly, the locations of $(n - k)$non-neighbor anchor nodes (as shown in Fig. 7 C_1, $C_2 \ldots C_{n-k}$) are stored in $(n - k)$ node units to be taken. Then, take any node from the units to form a triangle with two neighbor anchor nodes. According to [25], the more the triangle formed by these three nodes resembles a regular triangle, the smaller the localization error is. Furthermore, according to (16) and (17), the group with minimum δ was selected as the optimal group of anchor nodes, as shown in Fig. 7. By traversing $(n - k)$ non-neighbor anchor nodes, it can be discovered that C_1 is the optimum point, and it is hence recorded as C' for follow-up research. The distances between the anchor nodes on the projection plane are L_1, L_2, L_3. In this way, the current situation can be transformed into the situation of $K = 3$.

$$\mu = \frac{L_1 + L_2 + L_3}{3} \tag{16}$$

$$\delta = \sqrt{\frac{(L_1 - \mu)^2 + (L_2 - \mu)^2 + (L_3 - \mu)^2}{3}} \tag{17}$$

Besides, it is notable that the projection distances between the unknown node $P(x_P, y_P)$ and the two neighbor anchor

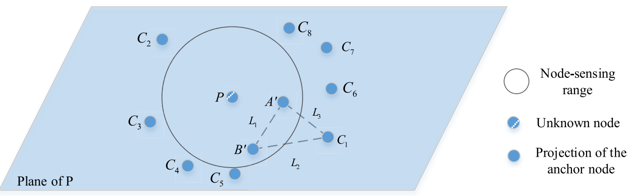

FIGURE 7. The position relation between anchor node and unknown node of $K = 2$.

nodes $A'(x_1, y_1)$, $B'(x_2, y_2)$ can be obtained by (9), but the projection distance between the unknown node and the non-neighbor anchor node cannot be obtained directly, so a triangular cosine algorithm based on spatial projection is proposed.

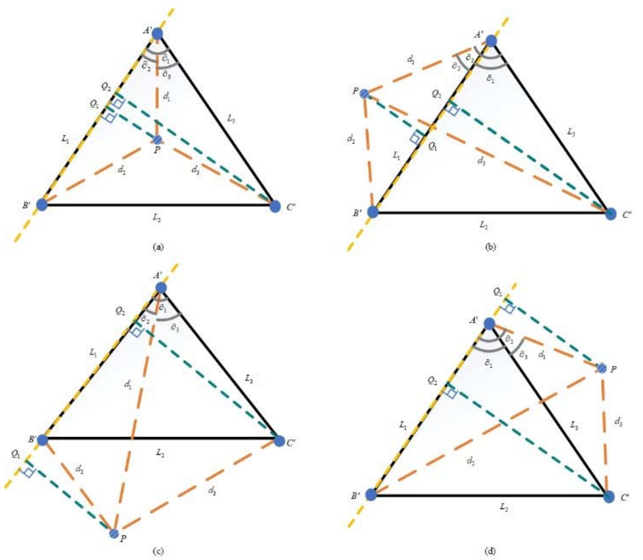

FIGURE 8. 2D location relation between the unknown node and anchor node.

As is shown in Fig. 8, there are four positional relationships between the unknown node P and the projections of the anchor nodes on the plane of the unknown node A', B', and C'. Through the comparative analysis of these four cases, we can get the particularity of angle relations to compute the distance. The vertical line between the non-neighbor anchor node C' and the straight line of the two neighbor anchor nodes $A'B'$ is $C'Q_2$, and the vertical line between the unknown node P and the straight line of the two neighbor anchor nodes $A'B'$ is PQ_1. In Fig. 8(a), (c), and (d), we can see the verticals PQ_1 and $C'Q_2$ are in the same direction. But, in the condition of Fig. 8(b), it can be seen that PQ_1 and $C'Q_2$ are in the opposite direction. The detailed analysis is described below:

When the horizontal and vertical coordinates of anchor nodes $A'(x_1, y_1)$ and $B'(x_2, y_2)$ are not equal and not in the same line with the unknown node, the equation of the line formed by these two nodes is as follows:

$$y - y_1 = \frac{(y_1 - y_2)}{(x_1 - x_2)}(x - x_1) \tag{18}$$

The equation of the line that passes through the unknown node $P(x_P, y_P)$ and the anchor node C', and are perpendicular to the line $A'B'$ are expressed as follows:

$$y - y_p = -\frac{(x_1 - x_2)}{(y_1 - y_2)}(x - x_p) \tag{19}$$

$$y - y_3 = -\frac{(x_1 - x_2)}{(y_1 - y_2)}(x - x_3) \tag{20}$$

Computing (18) and (19), the intersection coordinate $Q_1(x_{Q_1}, y_{Q_1})$ can be calculated. In a similar way, according to (18) and (20), we can get the intersection coordinate $Q_2(x_{Q_2}, y_{Q_2})$. In consequence, the direction vector of the vertical PQ_1 is $(x_P - x_{Q_1}, y_P - y_{Q_1})$ and the direction vector of the vertical $C'Q_2$ is $(x_3 - x_{Q_2}, y_3 - y_{Q_2})$.

Let $\mu = (x_P - x_{Q_1})\big/(x_3 - x_{Q_2})$. When it satisfies the condition of $\mu \leq 0$, the conclusion that the verticals PQ_1 and $C'Q_2$ are in the opposite direction is proposed; When it satisfies the condition of $\mu > 0$, the verticals PQ_1 and $C'Q_2$ are in the same direction. Similarly, when the horizontal and vertical coordinates of the anchor nodes A' and B' are equal, we can draw the same conclusion.

When $\mu \leq 0$, as shown in Fig. 8(b), ∂_1 is the angle between L_1 and L_3, ∂_2 is the angle between L_1 and d_1, and ∂_3 is the angle between L_3 and d_1.The relationship of the three angles in the Fig. 8(b) is:

$$\partial_3 = \partial_2 + \partial_1 \tag{21}$$

When $\mu > 0$, the relationship of the three angles in the Fig. 8(a), (c), and (d) is:

$$\partial_3 = |\partial_1 - \partial_2| \tag{22}$$

Moreover, ∂_1, ∂_2 can be known by Law of Cosines, and there are the following expressions:

$$\partial_1 = arccos\,\frac{L_1^2 + L_3^2 - L_2^2}{2L_1L_3} \tag{23}$$

$$\partial_2 = arccos\,\frac{d_1^2 + L_3^2 - d_2^2}{2d_1L_3} \tag{24}$$

∂_3 can be obtained by the formula above. Therefore, the projected distance d_3 between the unknown node P and the non-neighbor anchor node C can be obtained by (25).

$$d_3 = \sqrt{L_3 + d_1^2 - 2 \cdot L_3 \cdot d_1 \cdot cos\partial_3} \tag{25}$$

Finally, the unknown node coordinates can be estimated by (10)-(15).

4) $K = 1$

When the unknown node can only receive the location information of one neighbor anchor node, this paper proposes an auxiliary localization algorithm based on the node movement model.

In a 3D underwater environment, nodes can move actively along the anchor chain and be moved passively, according to the water current. It is assumed that the anchor coordinates, the depths (using the pressure sensor), and the offset angles

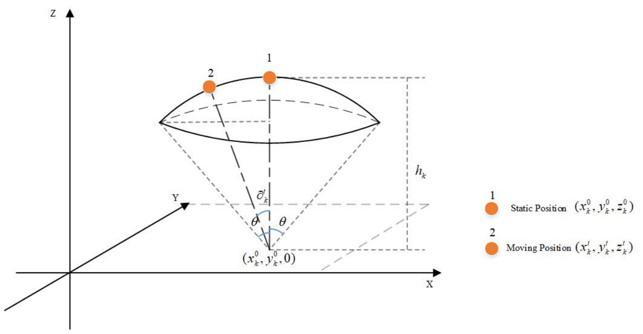

FIGURE 9. **Model of node movement.**

(using flow-transducer and angle sensor) of every anchor node can be obtained [26]. Influenced by the water current, the anchor node is highly likely to be offset from its static position. The mobility model of nodes is described as a type of node motion on spherical surfaces [26], as is shown in Fig. 9. The coordinate of the anchor node at time t is $P_k^t = (x_k^t, y_k^t, z_k^t)$. It is assumed that in the stationary position 1, the coordinate of an anchor node at time $t = 0$ is (x_k^t, y_k^t, z_k^t). The coordinate of the node in the moving position 2 at time t is $P_k^t = (x_k^t, y_k^t, z_k^t)$, then

$$\begin{cases} x_k^t = x_k^0 + h_k sin\, \partial_k^t cos\, \varphi_k^t \\ y_k^t = y_k^0 + h_k sin\, \partial_k^t cos\, \varphi_k^t \\ z_k^t = \left| h_k cos\, \varphi_k^t \right| \end{cases} \tag{26}$$

where ∂_k^t is the vertical offset angle between the current position and the static position, φ_k^t is the horizontal offset angle. Notably, z_k^t is the depth of the anchor node h_k. More importantly, suppose the maximum resultant force acting on any node is equal, then no matter at any depth, the maximum offset angle θ of the underwater node is equal.

Therefore, based on the above model, at every regular interval Δt, the moving position of the anchor node is recorded, that is, the position information of the anchor node at different offset angles is recorded. It is also noteworthy that the anchor node farthest from the anchor node within the maximum offset angle range is selected as the reference node to avoid collinearity. At this point, with the assistance of the location information of the reference node, the situation of $K = 1$ is transformed into the situation of $K = 2$. Finally, the coordinates of unknown nodes are calculated using the algorithm in the condition of $K = 2$.

E. THE COMPLETE MLR ALGORITHM

To show the whole process of MLR more clearly, the detailed pseudo algorithm of MLR for 3D UWSNs is listed in Table 2 as follows.

Firstly, the unknown nodes with more than three anchor nodes in the communication range in a 3D environment are estimated. Then, when there are three anchor nodes within the communication range of unknown nodes, convert the 3D planar to 2D positioning planar. Nonetheless, when the number of anchor nodes within the communication range of unknown nodes is less than three, coordinates estimation cannot be carried out. Therefore, a dynamic position-assisted localization method based on the mobility of the anchor nodes and neighbor anchor nodes is adopted. Besides, we propose a triangular cosine method to compute the 2D distance between the anchor node and the unknown node.

IV. SIMULATION RESULTS

A. SIMULATION SETTINGS

To verify the performance of the proposed scheme, three groups of simulations have been conducted in MatlabR2019b. The MLR algorithm is then compared with algorithms including the traditional ranging localization algorithm (i.e. the random deployment of the anchor node and unknown node, the TOA algorithm for distance estimation and the least square method for coordinate estimation), MALS-TSF algorithm, and the MBIL algorithm. For convenience, the traditional ranging localization algorithm is named as TRLA in the following part.

One hundred independent tests are carried out to assess the performance of all methods. The anchor nodes are deployed on the vertex of the regular tetrahedron, and the unknown nodes are randomly deployed in the 3D environment. Both the anchor nodes and the unknown nodes are fixed by the cable; besides, the depths of the sensor nodes can be measured by the depth sensors. The setups of system parameters are given in Table. 3. The intention of selecting different number of anchors, different number of nodes and different communication ranges is to explore the localization performance of all algorithms in terms of the anchor proportion, the node density and the node connectivity. There are two main evaluation indexes:

Average localization error: the average difference between the estimated position and the real position of the node. It can be calculated by:

$$\text{Ave Error} = \frac{\sum_{j=1}^{m} \sqrt{(X_{P_j} - x_{P_j})^2 + (Y_{P_j} - y_{P_j})^2 + (Z_{P_j} - z_{P_j})^2}}{m * R} \tag{27}$$

Localization Rate: the ratio of the localized nodes' number to the total number of sensor nodes. It can be expressed as follows:

$$\text{LR} = \frac{m_L}{m} \tag{28}$$

where m_L is the number of unknown nodes being localized.

B. RESULTS ANALYSIS

1) LOCALIZATION RATE AND AVERAGE LOCALIZATION ERROR OF MLR

As depicted in Fig. 10 and Fig. 11, the localization rate and average localization error vary as the number of anchor nodes n changes. The communication range R is kept to 90 m and the total number of nodes is fixed at 300. The number of anchor nodes n varies from 10 to 50. According to the results of Fig. 10 and Fig. 11, with the increase of the number

TABLE 2. The pseudo code for MLR.

```
Algorithm: MLR
Input: the total number of nodes N, the number of anchors
    n and the communication range R
Generate regular tetrahedron deployment network topology;
for j=1:(N-n) do
  Anchor nodes broadcast position information;
  Unknown nodes receive position information;
  Compute the distance D between all nodes using (1);
  Record the number of anchor nodes within the communication range of unknown nodes;
  Preprocess collinearity phenomenon;
  Record the number of neighbor anchor nodes K;
  if K >= 4
    A group of four anchor nodes is used to judge whether a regular tetrahedron is formed until the end of traversal;
    Calculate the unknown node coordinates using (3) - (8);
  else if K = 3
    Project the three anchor nodes onto the plane of the unknown node;
    Compute the 2D distance d between the unknown node and anchor nodes using (9);
    Calculate the unknown node coordinates using (10) - (15);
  else if K = 2
    Project the two anchor nodes onto the plane of the unknown node;
    Select minimum δ as the optimal group of anchor nodes using (16)- (17);
    Calculate the 2D distance d between the unknown node and non-neighbor anchor node by the triangular cosine distance algorithm based on spatial using (18)- (25);
    Calculate the unknown node coordinates using (10) - (15);
  else if K = 1
    Record the moving location's coordinate of the anchor node as the time changes;
    Select the reference node;
    Project the anchor node and the reference node onto the plane of the unknown node;
    Select minimum δ as the optimal group of anchor nodes using (16)- (17);
    Calculate the 2D distance d between the unknown node and non-neighbor anchor node by the triangular cosine distance algorithm based on spatial using (18)- (25);
    Calculate the unknown node coordinates using (10) - (15);
  end if
end for
Output: the unknown node coordinate
```

TABLE 3. Simulation parameters.

Parameter Names	Values
Monitoring area(S)	300m × 300m × 300m
Communication range(R)	$70m \leq R \leq 110m$
Number of anchor nodes(n)	$10 \leq n \leq 50$
Total number of nodes(N)	$150 \leq N \leq 450$
Simulation times	100

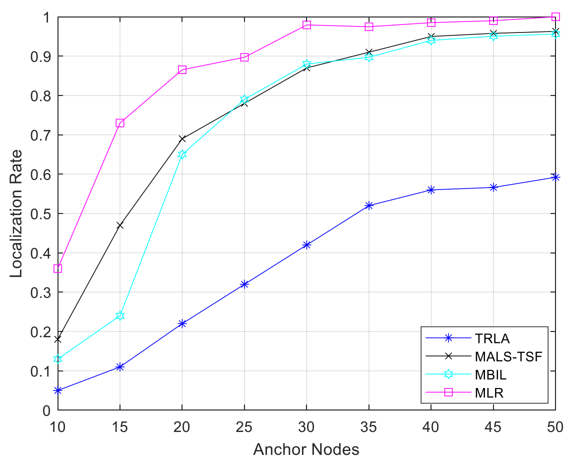

FIGURE 10. Localization Rate with different number of anchor nodes.

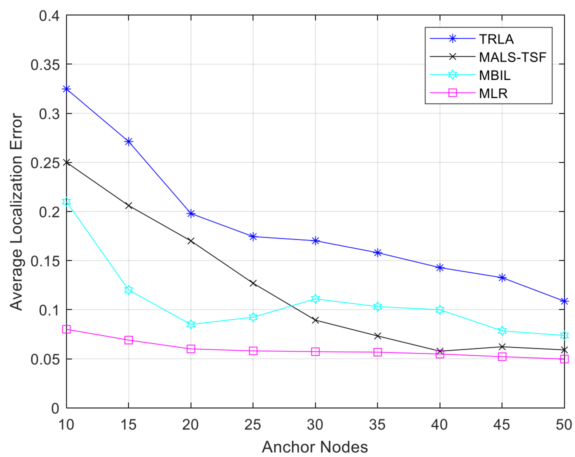

FIGURE 11. Average localization error with different number of anchor nodes.

of anchor nodes n, the localization rate tends to rise and the average localization error decreases for all algorithms. This is because with the increase of the anchor nodes, more unknown nodes can receive the messages broadcasted by more anchor nodes, thus being located. In Fig. 10, when the number of anchor nodes reaches 40, the node location rate reaches more than 90% except for TRLA. This is because TRLA can only estimate the coordinates when the number of neighbor anchor nodes around the unknown node is not less than three, while the other three methods improve this with different strategies to increase the node location rate. Moreover, MLR algorithm can guarantee the superiority of node positioning rate while ensuring high positioning accuracy.

Fig. 12 and Fig. 13 show the localization rate and average localization error of nodes vary with the communication

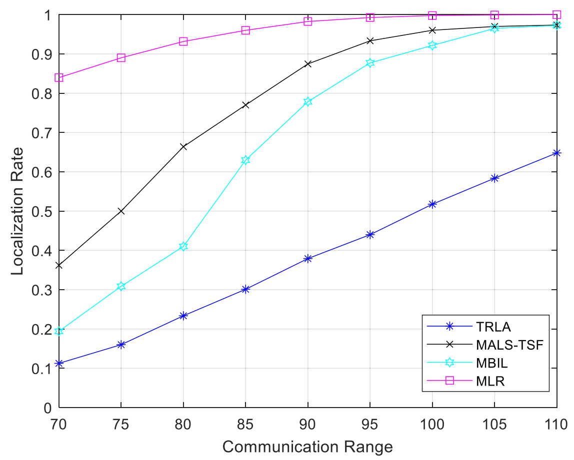

FIGURE 12. Localization Rate with different communication range.

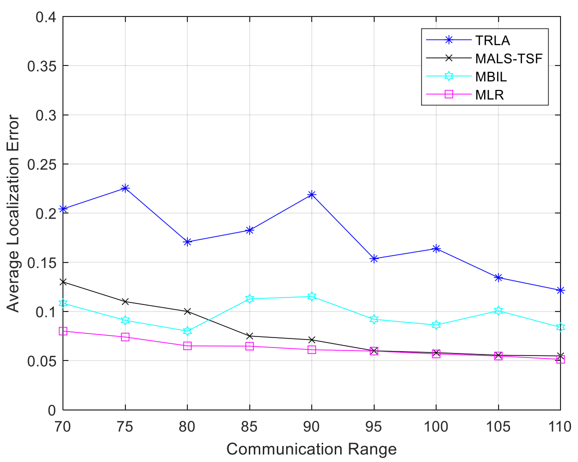

FIGURE 13. Average localization error with different communication range.

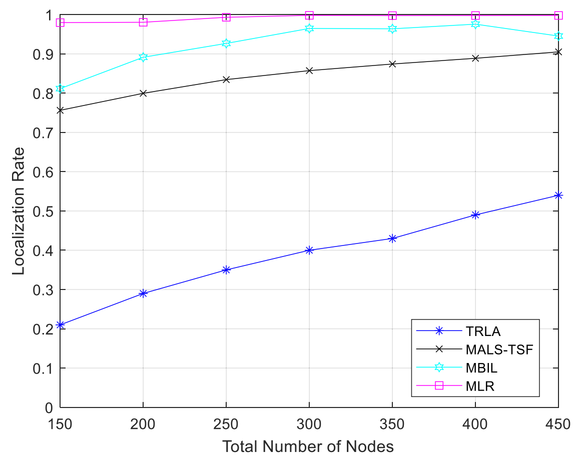

FIGURE 14. Localization Rate with different number of the total nodes.

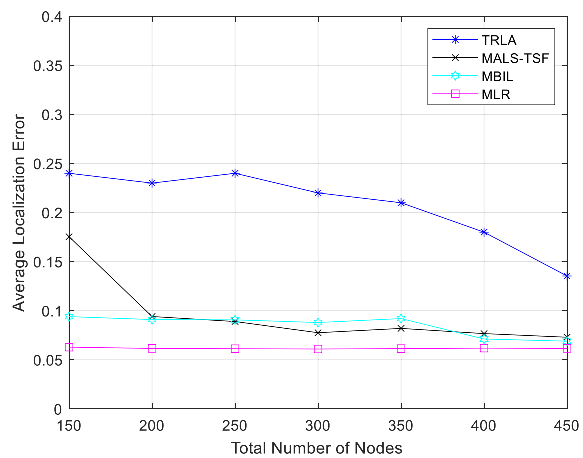

FIGURE 15. Average localization error with different number of the total nodes.

range R of nodes. To analyze the influence of different R on the localization rate, the number of anchor nodes n is fixed at 30 and the total number of nodes is fixed at 300, then R varies from 70 m to 110 m. As shown in Fig. 12, the localization rates will rise with the increase of R. This is because with the increase of communication range, the number of anchor nodes within the communication radius of unknown nodes raises. It can be also seen that when the communication radius of nodes is 70, the node location rate of MLR can reach more than 80%, while other algorithms only reach 40%. The reason for the above phenomenon is that when the communication radius of nodes is small, the number of neighbor anchor nodes around unknown nodes is less than 3 in many cases, so the advantage of MLR algorithm is more obvious. In Fig. 13, with the increase of R, the average localization error of the MLR algorithm decreases gradually. Besides, compared with other algorithms, MLR has the lowest average positioning error.

In the results shown in Fig. 14 and Fig. 15, the localization rate of nodes varies with the total number of nodes N. To analyze the influence of different N on localization rate, the number of anchor nodes n is fixed at 30 and communication range R is fixed at 90 m, then N varies from 150 to 450. As shown in Fig. 14, the localization rates rise as N increases. This is because, with the increase in node density, the number of anchor nodes that can communicate around the unknown node rises as well. The MLR algorithm solves the problem of node marginalization, so all nodes, except the isolated ones can be located even if the N is small. Moreover, compared with other algorithms, the average localization error of the MLR algorithm is smaller and more stable, which can be seen from Fig. 15.

2) COMPLEXITY ANALYSIS OF MLR ALGORITHM

The time complexity does not specifically represent the actual execution time of the code, but rather the trend of code execution time as the size of the data increases. The time complexity of the four algorithms is shown in the Table. 4. Assuming the UWSNs consist of N sensor nodes and the number of anchors is n. Firstly, all algorithms adopt a range-based location algorithm in the stage of distance estimation. MALS-TSF uses the state analysis of mobile anchor nodes and ordinary sensor nodes and the two-way TOA method

TABLE 4. Complexity analysis of MLR.

Localization Method	Distance Estimation	Coordinate Estimation
TRLA	$O((N-n)\cdot n)$	$O(m'\cdot(N-n))$
MALS-TSF	$O((N-n)\cdot n)$	$O(m'\cdot(N-n)+l\cdot u)$
MBIL	$O((N-n)\cdot n)$	$O(m'\cdot(N-n)+l\cdot u\cdot p)$
MLR	$O((N-n)\cdot n)$	$O(C_{m'}^{4}\cdot(N-n))$

to measure the distance between the ordinary node and the anchor node. Also, MBIL uses the state analysis of mobile anchor nodes and ordinary sensor nodes and a stratification effect compensation method to estimate the distance between two sensor nodes. The MLR algorithm and TRLA use the two-way TOA method to estimate the distance. Although the methods are different, the time complexity of these four algorithms to calculate the distance between nodes is $O((N-n)\cdot n)$.

Secondly, in the stage of coordinate estimation, both the TRLA and the MLR algorithm complete the positioning only in one stage. MALS-TSF and MBIL divide the positioning into two stages. The located nodes in the first stage can be upgraded to reference anchor nodes to locate the remaining unknown nodes. It is assumed that m' is the number of anchor nodes around the unknown node, l is the number of reference anchor nodes, u is the number of remaining unknown nodes, and p is the number of iterations. In TRLA, the time complexity of the maximum likelihood method to estimate the location of unknown nodes is $O(m'\cdot(N-n))$. The algorithm complexity is shown in Table.4, from which it can be seen that at this stage, the complexity of the MLR algorithm has the largest magnitude when selecting the combination of anchor nodes that constitute the regular tetrahedron, so its time complexity is $O(C_{m'}^{4}\cdot(N-n))$. Compared with the TRLA, the increase in the complexity of MALS-TSF depends on the communication between the reference nodes and the remaining location nodes. Moreover, the increase in the complexity of the MBIL algorithm depends on the number of iterations and the communication between the reference nodes and the remaining location nodes.

Finally, through the two-stage summary, we can see that the complexity of the MLR algorithm is relatively low than the others.

3) ENERGY COST ANALYSIS OF MLR ALGORITHM

Energy consumption directly affects the life cycle and cost of the whole monitoring system.

MALS-TSF and MBIL algorithms concentrate more energy on reference anchor nodes, which lead to the energy exhaustion and reduces the lifetime of the network. Therefore, the energy loss of the reference nodes is considered when evaluating the confidence value of reference nodes in MBIL. Even if the reference nodes with high residual energy are selected for coordinate estimation, the energy consumption of the nodes will increase with the increase of the number of iterations. However, in MLR algorithm, the unknown node that has obtained the location information does not need to be selected as the reference node, so it does not need to communicate again. Hence, the energy loss is smaller than MALS-TSF and MBIL algorithms.

To conclude, the localization rate of the MLR algorithm will be improved with the increase of n, R, and N. By handling the situation that there are less than three neighbor anchor nodes within the communication range of unknown nodes in a 3D environment, the MLR algorithm locates all unknown nodes except isolated nodes, which greatly improves node localization rate, and reduces the localization error while maintaining a rather low time complexity and energy consumption.

V. CONCLUSION

To deal with the situation that unknown nodes can only be successfully located when there are four or more neighbor anchor nodes around them in a 3D environment, this paper proposes an algorithm that can achieve complete localization except for isolated nodes, namely the maximum localization rate (MLR) algorithm. Unlike traditional algorithms, MLR is designed for 3D large-scale UWSNs. Considering the node's positioning error, this scheme deploys anchor nodes at the vertices of some prepositioned regular tetrahedrons. Firstly, the locations of unknown nodes with more than three anchor nodes in the communication range in a 3D environment are estimated. Then, the 3D planar is converted to 2D positioning planar to localize sensor nodes. Nonetheless, when the number of anchor nodes within the communication range of unknown nodes is less than three, the coordinate estimation cannot be carried out. Therefore, a dynamic position-assisted localization method based on the mobility of the anchor nodes and neighbor anchor nodes is adopted. Besides, we propose a triangular cosine method to compute the 2D distance between the anchor node and the unknown node. Moreover, the simulation results show that, as the number of anchor nodes n, the total number of nodes N, and the communication range R of sensor nodes change, the MLR algorithm achieves a maximum localization rate effectively. However, the nodes' energy consumption should be taken into full consideration in the follow-up research.

ACKNOWLEDGMENT

(Huilong Jin and Jia Song are co-first authors.)

REFERENCES

[1] M. Nain, N. Goyal, L. K. Awasthi, and A. Malik, "A range based node localization scheme with hybrid optimization for underwater wireless sensor network," *Int. J. Commun. Syst.*, vol. 35, no. 10, Mar. 2022, doi: 10.1002/dac.5147.

[2] A. Toky, R. P. Singh, and S. Das, "Localization schemes for underwater acoustic sensor networks—A review," *Comput. Sci. Rev.*, vol. 37, Aug. 2020, Art. no. 100241, doi: 10.1016/j.cosrev.2020.100241.

[3] M. Shalaby, M. Shokair, and N. W. Messiha, "Performance enhancement of TOA localized wireless sensor networks," *Wireless Pers. Commun.*, vol. 95, no. 4, pp. 4667–4679, Apr. 2017, doi: 10.1007/s11277-017-4112-8.

[4] H. Xiong, M. Peng, S. Gong, and Z. Du, "A novel hybrid RSS and TOA positioning algorithm for multi-objective cooperative wireless sensor networks," *IEEE Sensors J.*, vol. 18, no. 22, pp. 9343–9351, Nov. 2018, doi: 10.1109/JSEN.2018.2869762.

[5] F. Jiang and Z. Zhang, "An improved underwater TDOA/AOA joint localisation algorithm," *IET Commun.*, vol. 15, no. 6, pp. 802–814, Apr. 2021, doi: 10.1049/cmu2.12122.

[6] Y. Sun, F. Zhang, and Q. Wan, "Wireless sensor network-based localization method using TDOA measurements in MPR," *IEEE Sensors J.*, vol. 19, no. 10, pp. 3741–3750, May 2019, doi: 10.1109/JSEN.2019.2892652.

[7] R. Zhou, J. Chen, W. Tan, and C. Cai, "Sensor selection for optimal target localization with 3-D angle of arrival estimation in underwater wireless sensor networks," *J. Mar. Sci. Eng.*, vol. 10, no. 2, p. 245, Feb. 2022, doi: 10.3390/jmse10020245.

[8] G. Qiao, A. Muhammad, M. Muzzammil, M. Shoaib Khan, M. O. Tariq, and M. S. Khan, "Addressing the directionality challenge through RSSI-based multilateration technique, to localize nodes in underwater WSNs by using magneto-inductive communication," *J. Mar. Sci. Eng.*, vol. 10, no. 4, p. 530, Apr. 2022, doi: 10.3390/jmse10040530.

[9] M. Burtowy, M. Rzymowski, and L. Kulas, "Low-profile ESPAR antenna for RSS-based DoA estimation in IoT applications," *IEEE Access*, vol. 7, pp. 17403–17411, 2019, doi: 10.1109/ACCESS.2019.2895740.

[10] Z. Zhang, C. Zhang, M. Li, and T. Xie, "Target positioning based on particle centroid drift in large-scale WSNs," *IEEE Access*, vol. 8, pp. 127709–127719, 2020, doi: 10.1109/ACCESS.2020.3008373.

[11] D. Han, Y. Yu, K.-C. Li, and R. F. de Mello, "Enhancing the sensor node localization algorithm based on improved DV-hop and DE algorithms in wireless sensor networks," *Sensors*, vol. 20, no. 2, p. 343, Jan. 2020, doi: 10.3390/s20020343.

[12] J. Chen, W. Zhang, Z. Liu, R. Wang, and S. Zhang, "CWDV-hop: A hybrid localization algorithm with distance-weight DV-hop and CSO for wireless sensor networks," *IEEE Access*, vol. 9, pp. 380–399, 2021, doi: 10.1109/ACCESS.2020.3045555.

[13] Y. Yuan, L. Huo, Z. Wang, and D. Hogrefe, "Secure APIT localization scheme against sybil attacks in distributed wireless sensor networks," *IEEE Access*, vol. 6, pp. 27629–27636, 2018, doi: 10.1109/ACCESS.2018.2836898.

[14] W. Cheng, A. Thaeler, X. Cheng, F. Liu, X. Lu, and Z. Lu, "Time-synchronization free localization in large scale underwater acoustic sensor networks," in *Proc. 29th IEEE Int. Conf. Distrib. Comput. Syst. Workshops*, Jun. 2009, pp. 80–87, doi: 10.1109/ICDCSW.2009.79.

[15] X. Cheng, H. S. H. Shu, and Q. Liang, "A range-difference based self-positioning scheme for underwater acoustic sensor networks," in *Proc. Int. Conf. Wireless Algorithms, Syst. Appl. (WASA)*, Aug. 2007, pp. 38–43, doi: 10.1109/ICDCSW.2009.79.

[16] M. Isik and O. Akan, "A three dimensional localization algorithm for underwater acoustic sensor networks," *IEEE Trans. Wireless Commun.*, vol. 8, no. 9, pp. 4457–4463, Sep. 2009, doi: 10.1109/TWC.2009.081628.

[17] M. R. Dong, H. B. Li, R. R. Yin, Y. H. Qin, and Y. T. Hu, "Scalable asynchronous localization algorithm with mobility prediction for underwater wireless sensor networks," *Chaos Solitons Fractals*, vol. 143, Feb. 2021, Art. no. 110588, doi: 10.1016/j.chaos.2020.110588.

[18] Y. Zhang, J. Liang, S. Jiang, and W. Chen, "A localization method for underwater wireless sensor networks based on mobility prediction and particle swarm optimization algorithms," *Sensors*, vol. 16, no. 2, p. 212, Feb. 2016, doi: 10.3390/s16020212.

[19] W. Zhang, G. Han, X. Wang, M. Guizani, K. Fan, and L. Shu, "A node location algorithm based on node movement prediction in underwater acoustic sensor networks," *IEEE Trans. Veh. Technol.*, vol. 69, no. 3, pp. 3166–3178, Mar. 2020, doi: 10.1109/TVT.2019.2963406.

[20] J. Luo, Y. Yang, Z. Wang, Y. Chen, and M. Wu, "A mobility-assisted localization algorithm for three-dimensional large-scale UWSNs," *Sensors*, vol. 20, no. 15, p. 4293, Jul. 2020, doi: 10.3390/s20154293.

[21] R. Li, H. Yin, J. Wang, and L. Jing, "Study on node localization of underwater sensor networks based on node dynamic selection and movement prediction," in *Proc. 13th Int. Conf. Commun. Softw. Netw. (ICCSN)*, Jun. 2021, pp. 1–5.

[22] Y. Su, L. Guo, Z. Jin, and X. Fu, "A mobile-beacon-based iterative localization mechanism in large-scale underwater acoustic sensor networks," *IEEE Internet Things J.*, vol. 8, no. 5, pp. 3653–3664, Mar. 2021, doi: 10.1109/JIOT.2020.3023556.

[23] G. Han, C. Zhang, L. Shu, and J. J. P. C. Rodrigues, "Impacts of deployment strategies on localization performance in underwater acoustic sensor networks," *IEEE Trans. Ind. Electron.*, vol. 62, no. 3, pp. 1725–1733, Mar. 2015, doi: 10.1109/TIE.2014.2362731.

[24] Y. Z. Zhang, S. Xiang, W. Y. Fu, and D. F. Wei, "Improved normalized collinearity DV-hop algorithm for node localization in wireless sensor network," *Int. J. Distrib. Sensor Netw.*, vol. 10, Jul. 2014, Art. no. 436891, doi: 10.1155/2014/436891.

[25] Y. Duan, H. Wang, and X. Qiao, "Sensor node localization based on RSSI ranging and grey wolf optimizer algorism in wireless sensor network," *Chin. J. Sens. Actuators*, vol. 12, pp. 1894–1899, Dec. 2018.

[26] C. Liu, Z. Zhao, W. Qu, T. Qiu, and A. K. Sangaiah, "A distributed node deployment algorithm for underwater wireless sensor networks based on virtual forces," *J. Syst. Archit.*, vol. 97, pp. 9–19, Aug. 2019, doi: 10.1016/j.sysarc.2019.01.010.

JIA SONG is currently pursuing the M.S. degree with the School of Software Engineering, Hebei Normal University, China. Her current research interest includes localization in wireless networks.

HUILONG JIN received the Ph.D. degree from Yanshan University. He is currently the President and a Professor at Hebei Normal University. His research interests include vocational education and electronic information.

XIAOBO SHEN received the Ph.D. degree from the College of Control Theory and Control Engineering, Zhengzhou University. His research interests include embedded systems and control and localization in wireless sensor networks.

SHUJING ZHANG received the Ph.D. degree from the College of Information Science and Engineering, Ocean University of China. Her research interests include SLAM for AUVs, computer vision, signal processing, underwater acoustic networks, and localization in wireless sensor networks.